*Atmósfera (1993)*, 6, *pp. 255-272*

# A model study of the time evolution of climate at the secular time scale

I. SMITS, TH. FICHEFET, CH. TRICOT*, and J.-P. VAN YPERSELE

*Université Catholique de Louvain, Institut d'Astronomie et de Géophysique G. Lemaître*
*2, chemin du Cyclotron B-1348 Louvain-la-Neuve, Belgium*

(Manuscript received October 9, 1992; accepted in final form March 3, 1993)

RESUMEN

Se llevan a cabo experimentos numéricos con un modelo climático zonalmente promediado de dos dimensiones, para investigar la respuesta transitoria del clima del Hemisferio Norte, a los forzamientos solar y de gases de invernadero en la escala cronológica secular. La componente atmosférica del modelo se basa en el sistema de ecuaciones de vorticidad potencial casi geostrófica de dos niveles. En la superficie, el modelo incluye las áreas oceánicas y las terrestres, e incorpora los balances detallados de las masas de nieve y de hielo marino. El océano superior está representado por un modelo de capa mezclada integral, en el que la convergencia de calor está parametrizada por una ley difusiva.

Para la simulación de la respuesta transitoria del clima, a los forzamientos continuamente cambiantes, el ingreso de las perturbaciones térmicas al océano profundo se aproxima como si fuera difusión vertical. Una comparación entre los climas presentes observados y calculados, muestra que el modelo funciona razonablemente bien, al simular los ciclos estacionales de varias variables climáticas. En los experimentos reportados aquí, tomamos en cuenta los cambios de la radiación solar, parametrizados a partir de observaciones recientes de satélite, empleando el número de Wolf como base, así como las variaciones en la radiación solar causadas por los cambios en los elementos orbitales de la Tierra. En los primeros de estos experimentos se induce con nuestro modelo un calentamiento de cerca de 0.005 K entre los intervalos 1765-1875 y 1876-1990, mientras que los cambios en los elementos orbitales, son responsables de un enfriamiento de cerca de 0.003 K.

ABSTRACT

Numerical experiments are carried out with a two-dimensional zonally averaged climate model in order to investigate the transient response of the climate of the Northern Hemisphere to the solar and greenhouse-gas forcings at the secular time scale. The atmospheric component of the model is based on the two-level quasi-geostrophic potential vorticity system of equations. At the surface, the model has land–sea resolution and incorporates detailed snow and sea-ice mass budgets. The upper ocean is represented by an integral mixed-layer model in which meridional convergence of heat is parameterized by a diffusive law. For the simulation of the transient response of climate to continuously changing forcings, the uptake of heat perturbations by the deep ocean is approximated as vertical diffusion. A comparison between the computed and observed present climates shows that the model does reasonably well in simulating the seasonal cycle of various climatic variables. In the experiments performed here, we consider the solar irradiance changes, parameterized from recent satellite observations using the Wolf number as a basis, as well as the variations in solar radiation caused by the changes in the Earth's orbital elements. The former induces in our model a warming of about 0.005 K between the time intervals 1765–1875 and 1876–1990, while the latter is responsible for a cooling of about 0.003 K. These changes appear weak compared to the greenhouse-gas-induced warming simulated by the model.

* Present affiliation: Institut Royal Météorologique de Belgique, Départment de Climatologie, Avenue Circulaire 3, B–1180 Bruxelles, Belgique

## 1. Introduction

The study of the natural variability of climate is a fundamental subject when one wants to quantify the impact of human activities on the Earth's climate. There are, in fact, a number of different natural forcings and internal processes that can induce climatic changes at the annual to century time scales, like changes in the solar irradiance, variations in the concentration of atmospheric aerosols due to volcanic activity, modifications in the cloud amount and radiative properties, or changes in the global ocean circulation (Hougthon *et al.*, 1990).

In addition to the increase of human-induced greenhouse gases, the variations of the solar luminosity and volcanic activity have been the most investigated forcings because the physical basis of their link with climate is relatively well established. Two approaches, based respectively on physical modelling and statistical analysis, are usually used to elucidate the relative importance of these external factors on the climate of the past century. In order to determine in a physically-based manner the relative importance of the external forcings in producing the observed temperature record, several energy-balance climate models have been used to simulate the time evolution of the global mean surface temperature of the Earth over the last century (e.g., Hansen *et al.*, 1981; Gilliland, 1982; Wigley and Raper, 1990). It can be concluded from these studies that an accurate knowledge of the past climate forcings is essential for such a modelling work. The statistical approach tries to verify the alleged relationship between a particular forcing and climatic (especially, temperature) time series using various correlation techniques. In particular, multiple regression analysis allows to study the signal to noise ratio for combinations of various forcing parameters (e.g., Cress and Schönwiese, 1992). It is well recognized that the statistical findings should not be overinterpreted, but seen in context with deterministic results. In particular, statistical studies can help to point to possible forcing mechanisms that (still) cannot be explained to a satisfactory degree by deterministic models.

Recently, secular changes in solar activity have been claimed to have a direct influence on global climate (e.g., Reid, 1991; Lean *et al.*, 1992). On the other hand, continuous satellite measurements of solar irradiance over the last 11-year activity cycle and observations of solar-type stars have reduced the uncertainties in the estimate of the solar radiative output changes at the secular time scale. These recent findings are at the origin of the present study.

The Sun is the dominant energy source of the climate system. Any change in the solar radiation received at the top of the atmosphere will therefore affect the Earth's climate. It is now well known that such changes occur at various time scales. At the geological time scale, the standard stellar evolution models show that the solar irradiance has uniformly increased (Newman and Rood, 1977). At the 10- to 100-kyr time scale, the variations in the Earth's orbital elements induce changes in the solar radiation that were responsible for the Pleistocene ice ages (Berger, 1988). Recent satellite data have confirmed that the Sun's irradiance (or solar constant) also varies on shorter time scales. The radiometers taken aboard satellites have shown that the total radiative output of the Sun varies by up to 0.2% in a week because of the Sun rotation (Foukal, 1990). At the 11-year cycle time scale, the spacecraft measurements have revealed a 0.1% decrease (about 1 $Wm^{-2}$) in the solar irradiance between the solar activity maximum in 1980 and the mid-1986 minimum (Willson and Hudson, 1988).

The main purpose of the present work is to evaluate with a two-dimensional zonally averaged climate model the role played by the solar forcings in the global surface warming observed since a century ($0.45 \pm 0.15$ K; Houghton *et al.*, 1992). We will consider the changes in solar irradiance associated with the solar magnetic activity as well as the variations in solar radiation due to the changes in the Earth's orbital elements. We will also investigate the combined effects of the solar forcings and the greenhouse effect perturbation reconstructed since the beginning of the industrial era. It is worth noting that the model used here exhibits no internal variability, which

allows an unequivocal quantitative assessment of the influence of the forcings mentioned above. Of course, this model peculiarity has to be borne in mind when extending the findings of the present study to the real world.

The paper is organized as follows. The climate model is described in Section 2. Section 3 compares selected results of a simulation of the present climate with observations. In Section 4, we examine the model transient response to the solar and/or greenhouse-gas forcings between the pre-industrial era and the present time. Concluding remarks are finally given in Section 5.

## 2. Model description

Our model is a two-dimensional zonally averaged climate model designed for simulating the seasonal cycle of the climate of the Northern Hemisphere (Gallée *et al.*, 1991). For all the experiments presented in this paper, a latitudinal resolution of 5 degrees is chosen.

The atmospheric component of the model is based on the zonally averaged form of the two-level quasi-geostrophic potential vorticity system of equations (including diabatic heating and frictional dissipation) written in spherical and pressure coordinates (Sela and Wiin-Nielsen, 1971; Ohring and Adler, 1978). The main output consists of the latitudinal distribution of the temperature at 500 hPa and of the zonal wind at 250 and 750 hPa. Meridional transport of quasi-geostrophic potential vorticity is accomplished by an eddy mixing process using exchange coefficients parameterized as in Gallée *et al.* (1991). It is well known that the quasi-geostrophic approximation leads to an underestimation of the strength of the Hadley cell in low latitudes and, therefore, to an overestimation of the temperatures in these regions (e.g., White and Green 1984). To partly remedy this problem, a parameterization of the vertically integrated Hadley heat transport (Peng *et al.*, 1987) has been introduced in the model. Separate surface energy balances are calculated over various surface types at each latitude (see below), and the heating of the atmosphere due to the vertical heat fluxes is the weighted average of the convergences of these fluxes above each kind of surface. The vertical heating processes considered are solar radiation, long-wave radiation, convection, and latent heat release.

The solar radiation scheme used here is very similar to the one described by Tricot and Berger (1988). The following processes are included: absorption by $H_2O$, $CO_2$, and $O_3$, Rayleigh scattering, absorption and scattering by cloud droplets and aerosols, and reflection by the Earth's surface. The long-wave radiation computations are based on Morcrette's (1984) wide-band formulation of the radiative transfer equation. Absorption by $H_2O$, $CO_2$, and $O_3$ is explicitly treated and the cloud cover is supposed to behave as a blackbody, as is the Earth's surface. In both schemes, account is taken of variation in surface topography.

A single cloud layer is assumed to exist in each latitude belt, with monthly cloud amount prescribed from zonal mean climatology. The base and top altitudes of the cloud layer and its optical thickness are kept fixed throughout the year. The surface fluxes of sensible and latent heat are parameterized according to Saltzman and Ashe (1976) and Saltzman (1980), respectively. Latent heat release in the atmosphere is obtained from observed zonal and monthly mean precipitation rates uniformly scaled to ensure a balance between precipitation and evaporation over the whole hemisphere. Above the Greenland ice sheet, precipitation rates are further modified to incorporate the effects induced by the distance to the moisture source and by the surface slope and elevation of the ice sheet (Oerlemans, 1982).

At each latitude, the model surface is resolved into continental and oceanic portions. Land can be partly covered by snow and by the Greenland ice sheet. The mean altitude of the ice-free land and the elevation and extent of the Greenland ice sheet are specified from data. Sea ice can exist at the ocean surface and varies in amount at the expense of the open water area.

Over the snow- and ice-free land, surface temperature is determined by an energy balance equation accounting for the subsurface heat storage (Taylor, 1976). The groundwater budget is computed by the so-called "bucket method" of Manabe (1969). The soil is assumed to have a water-holding capacity of 40 cm. If the calculated soil moisture exceeds this value, the surplus is supposed to run off. Changes in soil moisture depend on the rates of rainfall, evaporation, snow melt, and run-off. The fraction of the ice-free land area above which precipitation falls as snow, $f_{sf}$, is parameterized as a function of the surface temperature following Harvey (1988). As the surface temperature decreases, $f_{sf}$ increases but only a single average snow depth is stored. When $f_{sf}$ decreases from one time step to the next, the new snow is uniformly distributed over the existing snow-covered area. The surface temperature of the snow layer is obtained by assuming an equilibrium between the internal conductive heat flux and the other surface heat fluxes. When the predicted temperature reaches 0°C, snow melt occurs. This melting is partitioned between a decrease in snow extent and a decrease in snow depth, so that snow area is gradually reduced during the snow melt period. The Greenland ice sheet is supposed to be completely covered by perennial snow. The proportion of precipitation falling as snow over its surface is a function of the surface temperature as in Ledley (1985). An energy balance equation similar to the one applied for snow on land provides the temperature at the air-snow interface. The net accumulation rate of snow is derived from an explicit surface mass budget.

The upper ocean (up to a depth of 150 m) is represented by the variable depth and temperature mixed-layer model of Gaspar (1988). Meridional convergence of heat due to oceanic currents is modelled by a diffusive law according to Sellers (1973). In the presence of sea ice, the mixed-layer depth is fixed at 150 m. The surface temperature of the ice pack and the vertical ice growth and decay rates are computed by the zero-layer model of Semtner (1976). Snow on top of the ice layer is not taken into account and no dynamic effects, such as ice drifting caused by wind, are considered. The opening and closing of leads and the open water temperature are calculated following the techniques of Parkinson and Washington (1979), subject to small modifications described in Gallée *et al.* (1991). The heat flux from the ocean to the ice is computed by assuming that sea ice is in thermodynamic equilibrium with the water just below. Therefore, both the temperature at the base of the ice and the temperature of the under-ice water are supposed to be equal to the freezing point of sea water. In the model, the only physical mechanism that can disturb this equilibrium is a partial mixing between the under-ice water and the lead water. To maintain the ice-covered water at the freezing point, the heat flux from the ocean to the ice has to compensate exactly for that perturbation.

Separate albedos are calculated for each surface type. The albedo of land not covered by snow or ice is a function of the soil moisture content according to Saltzman and Ashe (1976). Over continental areas covered by forests, the snow albedo is set equal to 0.40 (Robock, 1980). Elsewhere, the snow albedo is dependent on the surface temperature and the snow age as in Danard *et al.* (1984). Values of 0.85 and 0.65 are assigned to the maximum and minimum albedos of dry snow, respectively. For melting snow, the upper and lower limits of the albedo are assumed to be 0.70 and 0.40, respectively. These albedos are corrected later on to include the effects of snow depth and solar zenith angle. The albedo of ice-free ocean under clear sky is parameterized as a function of the solar zenith angle after Briegleb and Ramanathan (1982). Under cloudy conditions, the sea surface has an albedo of 0.07. The albedo of sea-ice is supposed to vary linearly with surface temperature, from 0.70 at -10°C to 0.45 at 0°C. A solar zenith angle correction is also applied here (Robock, 1980).

Finally, it should be noted that, in the experiments with time-dependent forcings, we approximate as a diffusion process the flux of temperature anomalies from the mixed layer into the deep ocean (Hansen *et al.*, 1988; Tricot, 1989). The deep ocean, taken to be the water below the maximum allowable mixed-layer depth (i.e., 150 m), is divided into 13 layers of variable thick-

ness, with a total thickness of 3850 m. The latitude-dependent effective diffusion coefficient, $k$, is deduced from Hansen *et al.* (1984) and ranges from 0.2 $cm^2s^{-1}$ near the equator to 5 $cm^2s^{-1}$ in high latitudes, leading to an hemispheric mean value of about 1.5 $cm^2s^{-1}$. Note that $k$ is constant in time and in the vertical direction. It is obvious that this simple treatment of the deep ocean excludes the effects of natural variability associated with ocean dynamics and the possibility of switches between the basic modes of ocean circulation. Thus, it must be considered as being only a first step in studying the transient response of climate to continuously changing forcings.

## 3. Simulation of the present climate

The model described above was first employed to simulate the present climate of the Northern Hemisphere. This control experiment was carried out by assuming a $CO_2$ concentration of 330 ppmv. Referring to Willson *et al.* (1981), the solar irradiance was taken as 1368 $Wm^{-2}$. Starting from arbitrary initial conditions, the model was run until an equilibrium seasonal cycle was established. The equilibrium was supposed to be achieved when the annual hemispheric mean radiative balance at the top of the atmosphere became less than 0.01 $Wm^{-2}$. This was reached after 100 years of integration.

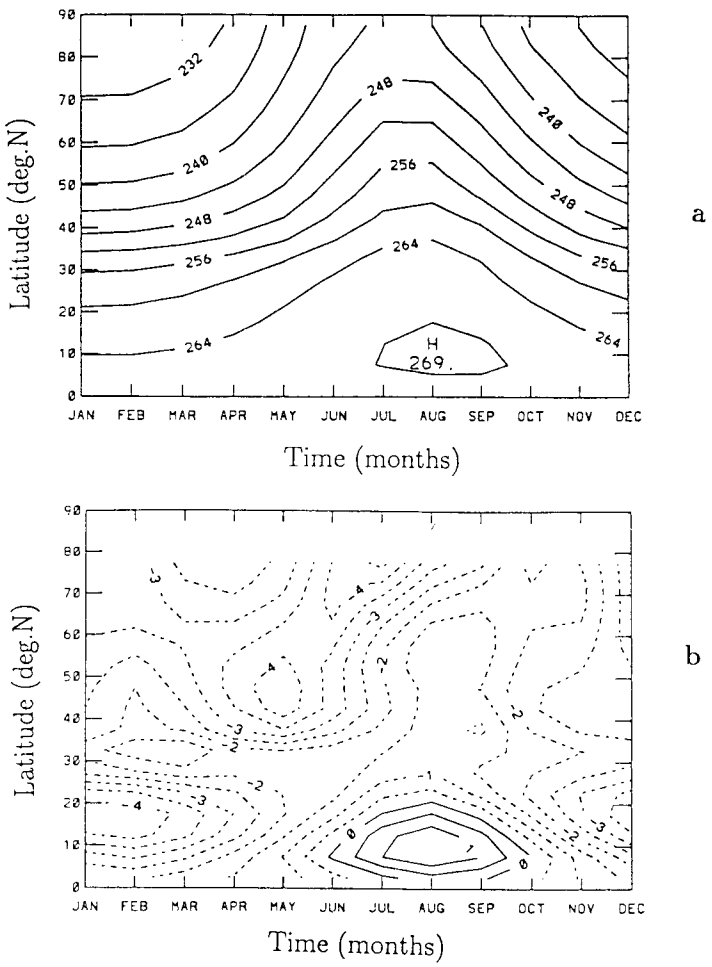


Fig. 1. Latitude-time distribution of the zonal mean temperature at 500 hPa simulated by the model (a) and of the difference between the computed temperature and the observations of Oort (1983) (b). Units are kelvins. The contour intervals are 4 and 0.5 K, respectively. Dashed line denotes negative deviation.

The seasonal cycle of the 500 hPa temperature simulated by the model is depicted in Figure 1a. The magnitude and horizontal gradient of temperature are in general agreement with the monthly mean data of Oort (1983). A plot of the difference between the estimated and observed temperatures in Figure 1b reveals that the major discrepancy occurs during winter in the tropics, where the modelled temperature is underestimated by 4 K. Reasons for this error stem basically from the limitations of the Hadley heat transport formulation. In the middle and high latitudes, the computed temperature is 3 to 4 K too low during spring and early summer. This deficiency is associated with an overestimation of the snow extent at the beginning of the melting period.

Figure 2a illustrates the seasonal variation of the oceanic mixed-layer temperature predicted by the model. The departure of the modelled temperature from the observed one (Levitus, 1982) is displayed in Figure 2b. This figure shows that the temperature difference never exceeds 2 K in the tropics. Near 35°N, the mixed layer is 4 K too cold in winter and spring. The excessive divergence of the oceanic heat transport simulated by the model in this zone is partly responsible for this large temperature anomaly. In the vicinity of 50°N, the computed temperature is 4 K too high during the summer months. This feature is mainly attributed to an insufficient vertical

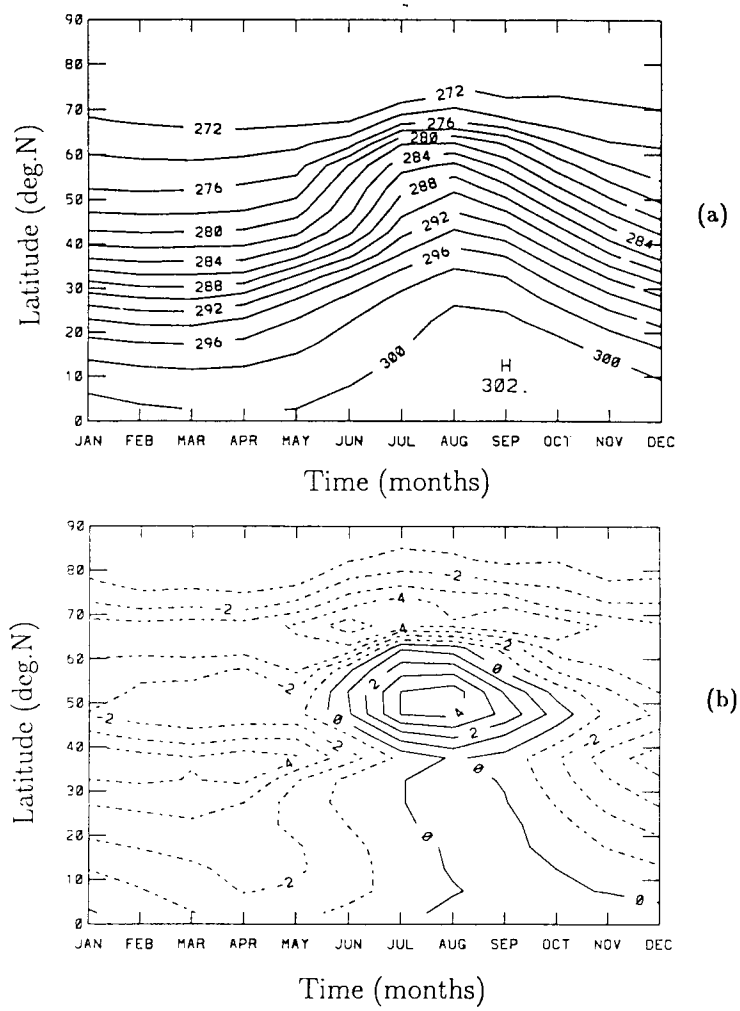


Fig. 2. Latitude-time distribution of the zonal mean sea-surface temperature simulated by the model (a) and of the difference between the computed temperature and the observations of Levitus (1982) (b). Units are kelvins. The contour intervals are 2 and 1 K, respectively. Dashed line denotes negative deviation.

mixing of the spring and summer surface heat input, which is due to an underestimation of the surface wind speed. Around 70°N, the model temperature is lower than observed by 4 to 5 K from May to October. An examination of the seasonal cycle of the sea-ice concentration simulated by the model indicates that the sea-ice compactness is overestimated at this latitude in spring. The overextensive ice cover prevents solar radiation from penetrating in the water, and thus delays and weakens the summer warming of the ocean. This effect, together with an exaggerated divergence of the ocean heat transport in fall, explain most of the temperature discrepancy. North of 80°N, the mixed layer remains close to the freezing point throughout the year, in agreement with data.

Because of its high albedo and insulating property, sea ice plays a crucial role in the energy balance of the climate system. Therefore, a necessary condition for a reliable numerical prediction of climate change is that the sea-ice simulation in the control run is realistic (Wilson and Mitchell, 1987). The comparison between the modelled seasonal cycle of the total sea-ice area and observations of Robock (1980) in Figure 3 shows that the phase of the seasonal variation is well reproduced. However, there tends to be too little ice from September to January and slightly too much in March and April. The use of a finer latitudinal resolution might reduce this problem (e.g., Harvey, 1986).

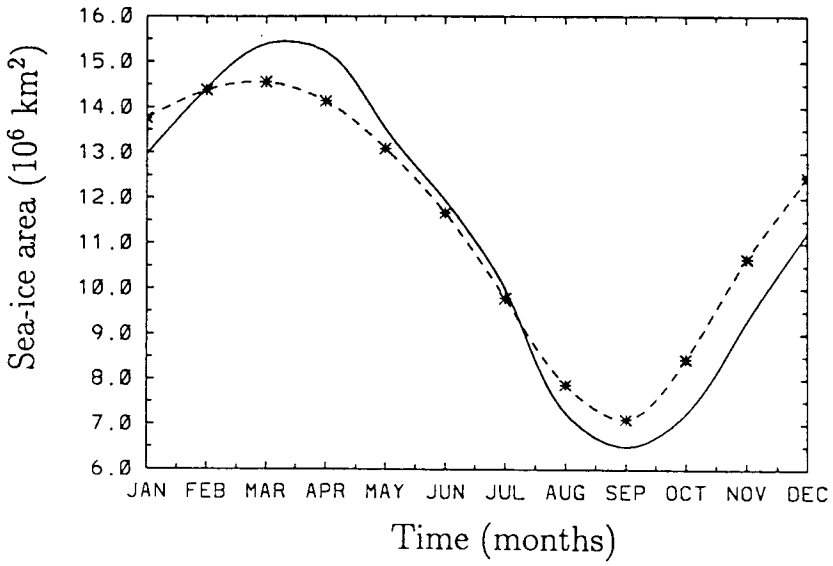


Fig. 3. Seasonal cycle of the total sea-ice area simulated by the model (solid curve) and observed following Robock (1980) (dashed curve).

Further evidence of the model performance for the present climate is given in Gallée *et al.* (1991). That paper demonstrates that the model shows acceptably good agreement with enough aspects of the seasonal behaviour of the real climate system to permit useful studies of a range of possible environmental perturbations.

## 4. Simulation of the transient response of climate to the solar and greenhouse-gas forcings over the last three centuries

In this section, we examine the model transient response to the solar and greenhouse-gas forcings between the pre-industrial era and the present time. We consider the solar irradiance changes,

parameterized from recent satellite observations using the Wolf number as a basis, as well as the variations in solar radiation caused by the changes in the Earth's orbital elements. It should be noted that the model has a sensitivity for a $CO_2$ doubling of 2.2 K, which is in the lower range of current estimates (1.5 – 4.5 K; Houghton *et al.*, 1992).

In all the experiments presented here, an equilibrium climate solution was first established for the solar forcings and atmospheric composition corresponding to the year 1700. Using this solution as initial condition, the model was then integrated up to 1990, with the solar and/or greenhouse-gas forcings changing with time according to plausible reconstructions. During this stage of the experiments, the uptake of heat pertubations by the deep ocean was approximated as a vertical diffusion process (see Section 2). A decision had to be made regarding the reference level for the solar irradiance. This reference level is important because it determines the steady state about which any fluctuations resulting from forcing perturbations will occur. A related consideration is the "history effect". Since the climate system has a long memory, the post-1700 climate response depends to some degree on the forcing fluctuations prior to 1700. Wigley and Raper (1990) estimated the importance of both the choice of the reference level and the "history effect", considering four different scenarios for the solar irradiance changes before the starting date. They deduce that the "history effect" is a vital consideration during the first few decades, but becomes unimportant after about 30 years (see also Fichefet and Tricot, 1992). Here, the reference level for the solar irradiance was taken as 1366.9 $Wm^{-2}$. This value was obtained from the parameterization of Willson and Hudson (1988), using the Wolf number corresponding to the year 1700 (see Section 4.1). In order to avoid the possible "history effect", the various figures shown hereafter give the model results after 1765.

### *4.1 Response to the solar forcings*

A first experiment was performed to quantify the influence of the solar irradiance changes on the time evolution of climate at the secular time scale. In this experiment the orbital elements were kept fixed to their 1700 values and the $CO_2$ concentration was taken equal to 280 ppmv, i.e., its pre-industrial value (Houghton *et al.*, 1990). Willson and Hudson (1988) correlated, over the period 1980–1987, the ACRIM (Active Cavity Radiometer Irradiance Monitor) daily mean data of total solar irradiance, $S$, with the Wolf number, $R_Z$, and suggested the following relationship:

$$S = 1366.82 + 7.71\ 10^{-3} * R_Z \tag{4.1}$$

where $S$ is in $Wm^{-2}$. This parameterization was used here and assumed to be valid over the last three centuries. The Wolf number data were supplied by the Sunspot Index Data Center of Uccle, Belgium (Koeckelenbergh and Cugnon, 1992, personal communication).

The lower curve in Figure 4 shows the reconstructed solar irradiance between 1765 and 1990. The maximum variation over this time period is about 1.5 $Wm^{-2}$ ($\simeq$ 0.1%) and occurs during solar cycle 19 (around 1957). The upper curve in the same figure gives the time evolution of the annual and hemispheric mean surface temperature simulated by the model. A series of 11-year peaks is observed, with the largest amplitude (about 0.05 K) taking place around 1957. The maximum temperature change between the low irradiance period in the early 1800s and the higher values in the 1950s is about 0.07 K. It is larger over continents ($\simeq$ 0.08 K) than over ocean ($\simeq$ 0.06 K) since the latter has a stronger damping effect. The comparison between the two curves in Figure 4 indicates that the surface temperature follows the solar activity cycle with a small time delay. A detailed analysis of the model outputs reveals that this time delay

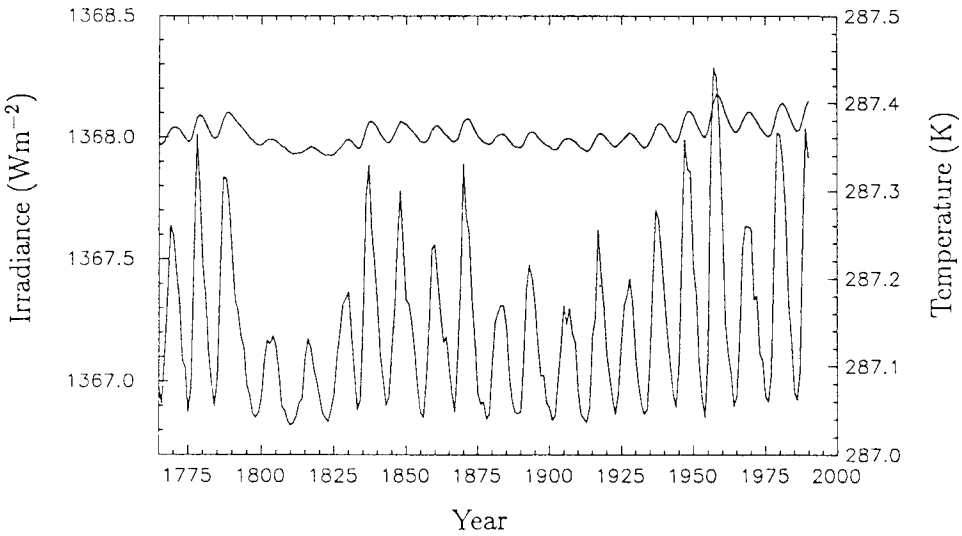


Fig. 4. Reconstructed solar irradiance changes (lower curve; see Section 4.1 for explanation) and time evolution of the annual and hemispheric mean surface temperature simulated in response to this forcing (upper curve). The solar irradiance at the starting date of model integration (the year 1700) is set equal to 1366.9 Wm$^{-2}$.

is fairly constant with latitude, despite the latitudinal variation of the oceanic heat diffusivity $k$ (see Section 2). In order to isolate a possible long-term temperature change in our simulation, we have computed the difference between the mean temperature of the time interval 1876–1990 and that of the time period 1765–1875. This difference amounts to + 0.0052 K and is therefore indicative of a weak warming trend. It is worth pointing that the time series of the latitudinal distribution of the modelled surface temperature change (not shown) indicates that the largest temperature variations are located at latitudes higher than 70°N during both warming and cooling periods. This behaviour is related to the amplification of the climate response due to the snow and ice albedo–temperature feedback. Figure 5a displays the time evolution of the annual mean total sea-ice area simulated by the model. The sea-ice area is maximum between 1795 and 1835, when the irradiance is rather weak. It is minimum around the year 1957, when the solar activity is maximum. Between the two time intervals chosen for averaging, the ice extent decreases by about 3,600 km$^2$ ($\simeq$ 0.03%). The continental snow area (Figure 5b) shows approximately the same behaviour.

A second experiment was carried out in which the solar irradiance and $CO_2$ concentration were kept fixed to their 1700 values, while the Earth's orbital elements were allowed to vary according to Berger (1978). The variations in these elements induce a decrease in the annual and hemispheric mean insolation received at the top of the atmosphere of only 0.0007 Wm$^{-2}$ between 1765 and 1990. Figure 6 demonstrates that the behaviour can be quite different for a particular month. For September, for example, there is a decrease in insolation of about 1 Wm$^{-2}$ over the time period considered.

The insolation variations mentioned above induce in the model an annual and hemispheric mean surface cooling of 0.0032 K between the two time intervals 1765–1875 and 1876–1990. The associated increase in sea-ice area amounts to about 0.2%. This large (compared to the previous experiment) change in sea-ice extent is related to the long-term decrease in insolation during the melting period.

It should be noted that an additional experiment was made by taking into account the time variations in both solar irradiance and Earth's orbital elements. The long-term response of the

annual and hemispheric mean surface temperature (+ 0.0017 K) obtained in this case is almost equal to the sum of the responses simulated in the first two experiments (+ 0.0020 K). Clearly, the solar forcings considered in the present study are unsufficient to explain the global surface warming observed since the late 19th century (0.45 ± 0.15 K; Houghton *et al.*, 1992).

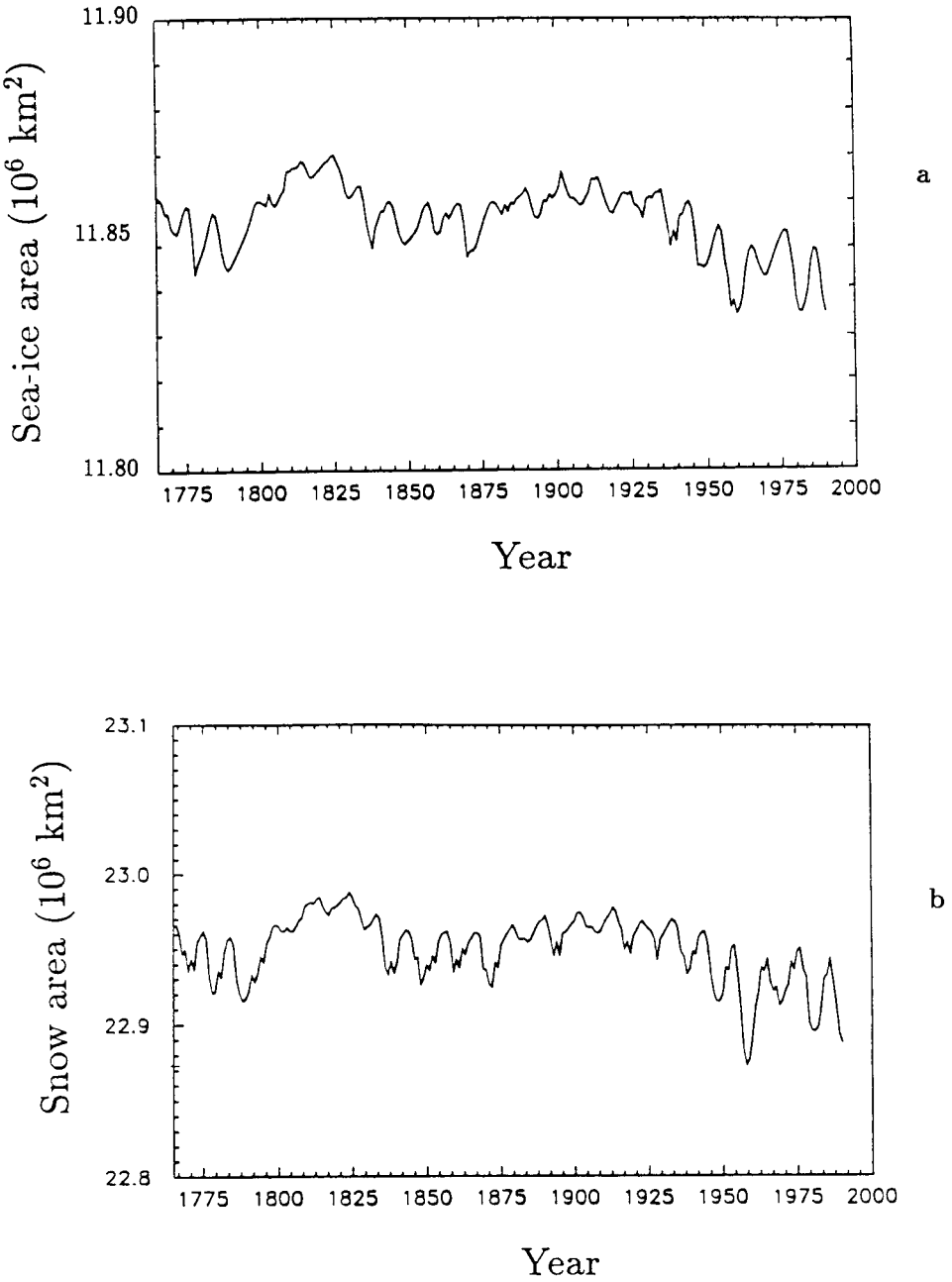


Fig. 5. Time evolution of the annual mean total sea-ice (a) and snow (b) areas in response to the solar irradiance changes depicted in Figure 4.

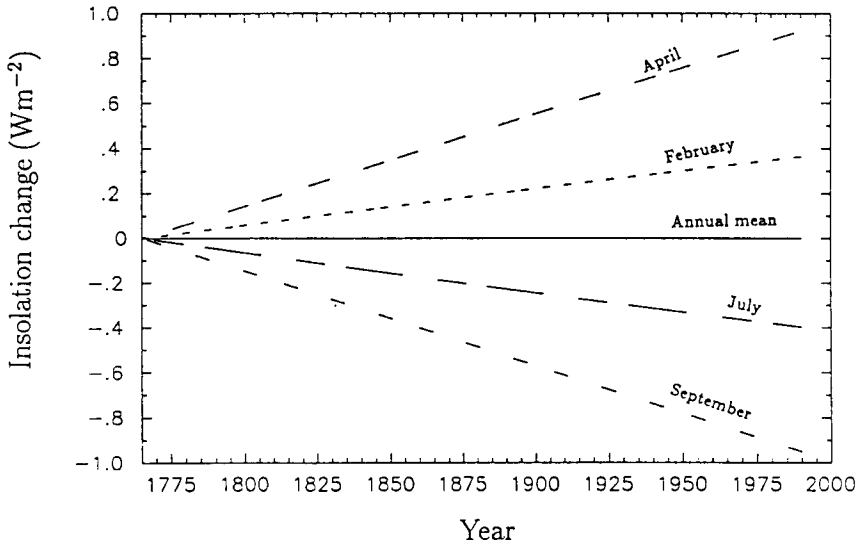


Fig. 6. Variations in the insolation received at the top of the atmosphere since 1765 due to the changes in the Earth's orbital elements (computed after Berger, 1978).

### *4.2. Response to the solar and greenhouse-gas forcings*

We now consider the solar effects superimposed on the forcing due to the gradual increase in greenhouse-gas concentrations. This forcing was expressed in terms of changes in equivalent $CO_2$ concentration. (The equivalent $CO_2$ concentration is the $CO_2$ concentration that would have the same radiative effect at the tropopause than the one caused by all the greenhouse gases, except water vapour). The time evolution of the equivalent $CO_2$ concentration between 1700

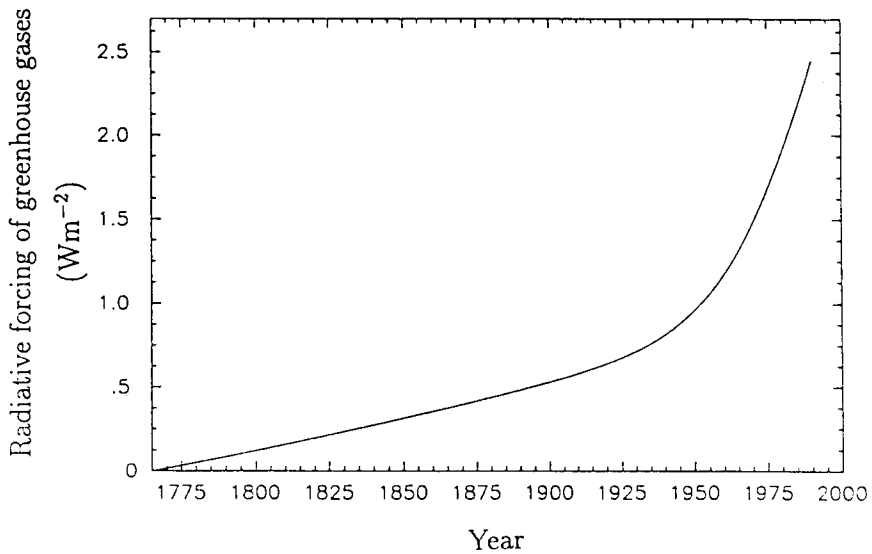


Fig. 7. Greenhouse-gas forcing history since 1765 following Houghton *et al.* (1990).

and 1990 was determined using concentration histories and concentration–forcing relationships for the most important greenhouse gases (i.e., $CO_2$, $CH_4$, $N_2O$, stratospheric $H_2O$, and CFCs) recommended by Houghton *et al.* (1990). The water vapour concentration is an internal model variable. The resulting radiative forcing at the tropopause is depicted in Figure 7. One notes an increase of about 2.5 Wm$^{-2}$ between 1765 and 1990. Two experiments were conducted with

the model submitted to this forcing. In the first one, the solar irradiance and the Earth's orbital elements were kept fixed to their 1700 values, while in the second one they were allowed to vary.

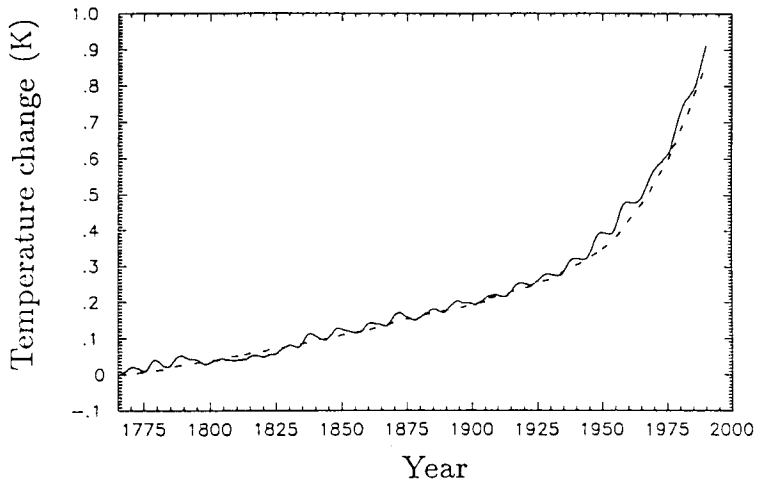


Fig. 8. Transient response of the annual and hemispheric mean surface temperature to the greenhouse-gas forcing alone (dashed curve) and to the solar and greenhouse-gas forcings taken together (solid curve). The solar forcings considered here are the solar irradiance changes associated with solar activity and the variations in the solar radiation caused by the changes in the Earth's orbital elements.

Figure 8 illustrates the transient response of the annual and hemispheric mean surface temperature simulated by the model with and without solar effects. It can be seen that the solar response shows up only as a minor perturbation. The surface warming produced by the model between 1765 and 1990 in the experiment with solar effects included amounts to about 0.9 K. Over the time interval 1890–1990, the temperature increase is about 0.7 K. This warming appears somewhat overestimated compared to the observed global temperature trend. Possible reasons for this discrepancy will be discussed in the concluding remarks. The transient response of the annual and zonal mean surface temperature for the experiment with solar effects accounted for is given in Figure 9. One sees that the warming rate increases with time and that the magnitude of the warming is maximum at latitudes higher than 70°N. The latter feature is, once

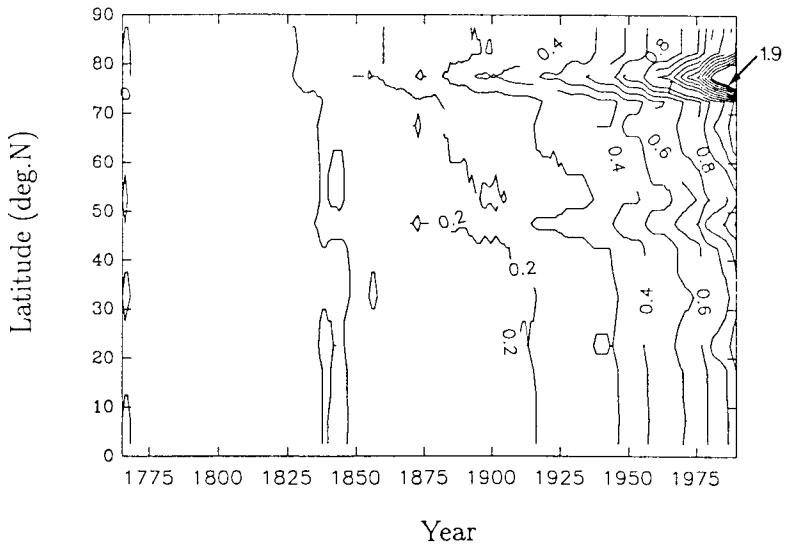


Fig. 9. Transient response of the annual and zonal mean surface temperature to the solar (see the remark in the legend of Figure 8) and greenhouse-gas forcings. The contour interval is 0.1 K. Units are kelvins.

again, a consequence of the snow and ice albedo–temperature feedback. Figure 10 shows that the computed annual mean sea-ice and snow areas decrease by about 7% over the time period 1765–1990.

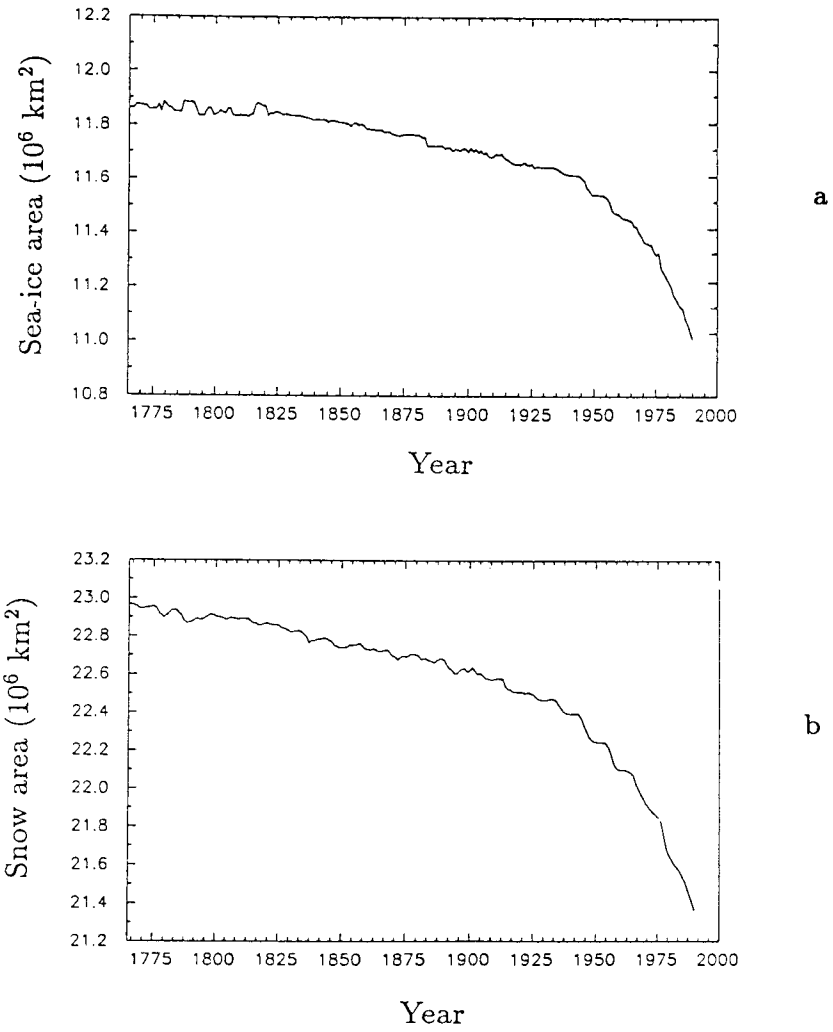


**Fig. 10.** Time evolution of the annual mean total sea-ice (a) and snow (b) areas in response to the solar (see the remark in the legend of Figure 8) and greenhouse-gas forcings.

The results of these two experiments indicate that a large part of the warming simulated by the model between 1765 and 1990 is induced by the build-up of greenhouse gases, the relative part of the solar forcings being extremely small.

## 5. Conclusion

Numerical experiments have been carried out with a two-dimensional zonally averaged climate model in order to evaluate the transient response of the climate of the Northern Hemisphere to the solar and greenhouse-gas forcings at the secular time scale. The different forcings considered in this study and the main results obtained are summarized in Tables 1 and 2, respectively.

Table 1. Magnitude of the forcings considered in the present work. For the solar and orbital forcings, the table gives the net downward radiation at the tropopause, while for the greenhouse-gas forcing, it gives the increase in net infrared radiation at the tropopause since 1765.

| Forcing type | Hemispheric forcing ($Wm^{-2}$) | | |
|---|---|---|---|
| | mean on 1765–1875 $\overline{Q}_1$ | mean on 1876–1990 $\overline{Q}_2$ | $\Delta\overline{Q}$ = $\overline{Q}_2$-$\overline{Q}_1$ |
| Solar activity (annual mean) | 231.3980 | 231.4070 | + 0.0090 |
| Orbital elements *annual mean | 231.3734 | 231.3733 | − 0.0001 |
| *February | 168.6042 | 168.7174 | + 0.1132 |
| *April | 254.9036 | 255.2022 | + 0.2986 |
| *July | 311.1247 | 310.9875 | − 0.1372 |
| *September | 239.6994 | 239.3793 | − 0.3201 |
| Greenhouse gases | 0.2000 | 0.9572 | + 0.7572 |

Table 2. Summary of the main results of the present study.

| Forcing type | Surface temperature (K) | | |
|---|---|---|---|
| | mean on 1765–1875 $\overline{T}_1$ | mean on 1876–1990 $\overline{T}_2$ | $\Delta\overline{T}$ = $\overline{T}_2$-$\overline{T}_1$ |
| Solar activity | 287.3620 | 287.3672 | + 0.0052 |
| Orbital elements | 287.3232 | 287.3201 | − 0.0032 |
| Greenhouse gases (GHG) | 287.3942 | 287.6733 | + 0.2791 |
| GHG + solar activity + orbitals elements | 287.4245 | 287.7163 | + 0.2918 |

Table 2 suggests, in accordance with Wigley and Raper (1990) and Gérard and Hauglustaine (1991), that the influence of solar irradiance changes on the hemispheric mean temperature is likely to be extremely weak, unless some other mechanism is operating beyond that leading to the photospheric effects incorporated in the Willson and Hudson (1988) parameterization. As noted by Foukal and Lean (1990), additional low frequency variations are possible given the absence of reliable irradiance data prior to the satellite era. Therefore, it will be interesting to reconsider this issue when the different missions planned during the following decades will have provided new data. Table 2 also shows that the changes in solar radiation due to the variations in the Earth's orbital elements have a very weak impact on the time evolution of climate at the secular time scale.

When the solar effects are combined with the forcing due to the build-up of greenhouse gases, our model simulates an annual and hemispheric mean surface warming of about 0.7 K between 1890 and 1990. Over the same time period, the observations shows a global temperature increase of 0.45 ± 0.15 K (Houghton *et al.*, 1992). Part of the discrepancy between the model and data could be due to an underestimation of the lag in the model response to external forcing changes. Indeed, our model has an *e*-folding time for an instantaneous $CO_2$ doubling of 13 years, which is in the lower range of current estimates (10–100 years; Schlesinger, 1989).

We will investigate this important point in the future by replacing the simple diffusive deep-ocean model used here by a zonally averaged three-basin ocean circulation model (Fichefet and Hovine, 1993). This change will also allow for the internal variability of climate associated with ocean dynamics and ocean–atmosphere interactions to be accounted for. It is worth noting that the absence of internal variability in the present version of the model could also be partly responsible for the disagreement mentioned above. Finally, we stress the fact that, in this study, we have not considered all the forcings that can influence the climatic system at the secular time scale. The concentration of stratospheric aerosols can be greatly enhanced over large areas for a few years following large explosive volcanic eruptions and can affect the Earth's radiative balance significantly (Shine *et al.*, 1990). In addition, it has long been recognized that tropospheric aerosols may exert a global cooling influence on climate, e.g., because of their scattering of shortwave radiation and the resultant increase in planetary albedo. Since 1850, industrial activities, especially emissions of $SO_2$, contributed to substantial local increases in the amount of tropospheric aerosols. However, the quantitative impact of these increases on the global radiative budget of the Earth is yet difficult to assess because the anthropogenic aerosols are distributed quite non uniformly over the Earth and are relatively short-lived (Charlson *et al.*, 1992).

**Acknowledgements**

We thank A. Koeckelenbergh and P. Cugnon for providing us with the Wolf number data. This research was partly supported by the Climate Programme of the Commission of the European Communities under contract EPOC-0003-C(MB). Th. Fichefet is sponsored by the National Fund for Scientific Research (Belgium). The National Fund for Scientific Research (Belgium) and the " Fonds de Développement Scientifique" of the "Université Catholique de Louvain" (Louvain-la-Neuve) supplied the computer time needed to complete the calculations. The graphics were made with the NCAR package.

REFERENCES

Berger, A., 1978. Long-term variations of daily insolation and quaternary climatic changes. *J. Atmos. Sc.*, **35**, 2362–2367.

Berger, A., 1988. Milankovitch theory and climate. *Rev. of Geophys.*, **26**, 624–657.

Briegleb, B., and V. Ramanathan, 1982. Spectral and diurnal variations in clear sky planetary albedo. *J. Appl. Meteor.*, **21**, 1160–1171.

Charlson, R. J., S. E. Schwartz, J. M. Hales, R. D. Cess, J. A. Coakley, J. E. Hansen, and D. J. Hofmann, 1992. Climate forcing by anthropogenic aerosols. *Science*, **255**, 423–430.

Cress, A., and C. D. Schönwiese, 1992. Statistical signal and signal-to-noise assessments of the seasonal and regional patterns of global volcanism–temperature relationships. *Atmosfera*, **5**, 31–46.

Danard, M., M. Gray, and G. Lyv, 1984. A model for predicting ice accretion and ablation in water bodies. *Mon. Weather Rev.*, **112**, 1160–1169.

Fichefet, Th., and S. Hovine, 1993. The glacial ocean: a study with a zonally averaged three-basin ocean circulation model. *Proceedings of the NATO-ARW on Ice in the Climate System.* In press.

Fichefet, Th., and Ch. Tricot, 1992. Influence of the starting date of model integration on projections of greenhouse-gas-induced climatic change, *Geophys. Res. Let.*, **19**, 1771–1774.

Foukal, P., 1990. Solar luminosity variations over timescales of days to the past few solar cycles. *Phil. Trans. R. Soc. Lond.,* **A330**, 591–599.

Foukal, P. and J. Lean, 1990. An empirical model of total solar irradiance variation between 1874 and 1988. *Science,* **242**, 556–558.

Gallée, H., J. P. van Ypersele, Th. Fichefet, Ch. Tricot, and A. Berger, 1991. Simulation of the last glacial cycle by a coupled, sectorially averaged climate–ice sheet model, I, The Climate Model. *J. Geophys. Res.,* **96**, 13,139-13,161.

Gaspar, Ph., 1988. Modelling the seasonal cycle of the upper ocean. *J. Phys. Oceanogr.,* **18**, 161–180.

Gérard, J. C., and D. A. Hauglustaine, 1991. Transient climate response to solar irradiance: reconstuction for the last 120 years. *Clim. Res.,* **1**, 161–167.

Gilliland, R. L., 1982. Solar, volcanic and $CO_2$ forcing of recent climatic changes. *Climatic Change,* **4**, 111–131.

Gilliland, R. L., and S. H. Schneider, 1984. Volcanic, $CO_2$ and solar forcing of Northern and Southern Hemisphere surface air temperatures. *Nature,* **310**, 38–41.

Hansen, J., I. Fung, A. Lacis, D. Rind, S. Lebedeff, R. Ruedy, G. Russell, and P. Stone, 1988. Global climate changes as forecast by Goddard Institute for Space Studies three dimensional model. *J. Geophys Res.,* **93**, 9341–9364.

Hansen, J., D. Johnson, A. Lacis, S. Lebedeff, P. Lee, D. Rind, and G. Russell, 1981. Climate impact of increasing atmospheric carbon dioxide. *Science,* **213**, 957–966.

Hansen, J., A. Lacis, D. Rind, G. Russell, P. Stone, I. Fund, R. Ruedy and J. Lerner, 1984. Climate sensitivity: analysis of feedback mechanisms. *Climate Processes and Climate Sensitivity, Geophys. Monogr. Ser.,* vol. **29**. Edited by J. E. Hansen and T. Takahashi, AGU, Washington, D.C., 130–163.

Harvey, L. D. D., 1986. A three-level energy balance climate model with topography, explicit radiative transfer, and explicit sea ice and snow mass budgets. Ph. D. Doctoral Thesis. University of Toronto, Ontario, Canada, 333 pp.

Harvey, L. D. D., 1988. A semianalytic energy balance climate model with explicit sea ice and snow physics. *J. of Climate,* **1**, 1065–1085.

Houghton, J. T., B. A. Callender, and S. K. Varney (Eds.), 1992. Climate Change 1992, The Supplement Report to the IPCC Scientific Assessment. Cambridge Univ. Press, Cambridge, 200 pp.

Houghton, J. T., G. T. Jenkins, and J. J Ephraums (Eds.), 1990. Climate Change, The IPCC Scientific Assessment. Cambridge Univ. Press, Cambridge, 364 pp.

Lean, J., A. Skumanich, and O. White, 1992. Estimating the Sun's radiative output during the Maunder minimum. *Geophys. Res. Let.,* **19**, 1591–1594.

Ledley, T. S., 1985. Sensitivity of a thermodynamic sea ice model with leads to time step size. *J. Geophys. Res.,* **90**, 2251–2260.

Levitus, S., 1982. Climatological Atlas of the World Ocean. *NOAA Prof. Paper 13.* U. S. Govt. Printing Office, Washington, D. C., 173 pp.

Manabe, S., 1969. The atmospheric circulation and the hydrology of the Earth's surface. *Mon. Weather Rev.,* **97**, 739–774.

Morcrette, J. J., 1984. Sur la paramétrisation du rayonnement dans les modèles de la circulation générale atmosphérique, Thèse de Doctorat d'Etat. Université des Sciences et des Techniques de Lille, Lille, 373 pp.

Newman, M. J., and R. T. Rood, 1977. Implications of solar evolution for Earth's early atmosphere. *Science,* **198**, 1035–1037.

Oerlemans, J., 1982. Response of the Antarctic ice sheet to a climate warming: a model study. *J. Climatol.,* **2**, 1–11.

Ohring, G., and S. Adler, 1978. Some experiments with a zonally-averaged climate model. *J. Atmos. Sci.,* **35**, 186–205.

Oort, A. H., 1983. Global atmospheric circulation statistics 1958–1973. *NOAA Prof. Paper 14.* Natl. Oceanogr. and Atmos. Admin., Washington, D.C., 180pp.

Parkinson, C. L., and W. M. Washington, 1988. A large-scale numerical model of sea ice. *J. Geophys. Res.,* **84**, 311–337.

Peng, L., M. D. Chou, and A. Arking, 1987. Climate warming due to increasing atmospheric $CO_2$: simulations with a multilayer coupled atmosphere-ocean seasonal energy balance model. *J. Geophys. Res.,* **92**, 5505–5521.

Reid, G. C., 1991. Solar total irradiance variations and the global sea surface temperature record. *J. Geophys. Res.,* **96**, 2835–2844.

Robock, A., 1980. The seasonal cycle of snow cover, sea ice and surface albedo. *Mon. Weather Rev.,* **108**, 267-285.

Saltzman, B., 1980. Parameterization of the vertical flux of latent heat at the Earth's surface for use in statistical-dynamical climate models. *Arch. Met. Geoph. Biokl., Ser. A,* **29**, 41–53.

Saltzman, B., and S. Ashe, 1976. Parameterization of the monthly mean vertical heat transfer at Earth's surface. *Tellus,* **28**, 323–331.

Schlesinger, M. E., 1989. Model projections of the climatic changes induced by increasing atmospheric $CO_2$. *Climate and Geo-Sciences, NATO-ASI series, 285.* Edited by A. Berger, S. Schneider, and J. C. Duplessy J. Cl., Kluwer Acad. Pub., Dordrecht, 375–415.

Schönwiese, C. D., 1984. Northern Hemisphere temperature statistics and forcing, Part B: 1579-1980 AD. *Arch. Met. Geophys. Biocl.,* **B35**, 155–178.

Sela, J., and A. Wiin-Nielsen, 1971. Simulation of the atmospheric annual energy cycle. *Mon. Weather Rev.,* **99**, 460–468.

Sellers, W. D., 1973. A new global climate model. *J. Appl. Meteorol.,* **22**, 1557–1574.

Semtner, A. J., 1976. A model for the thermodynamic growth of sea ice in numerical investigations of climate. *J. Phys. Oceanogr.,* **6**, 379–389.

Shine, K., R. G. Derwent, D. J. Wuebbles, and J. J Morcrette, 1990. Radiative forcing of climate, *Climate Change, The IPCC Scientific Assessment.* Edited by J. T. Houghton, G. J. Jenkins, and J. J. Ephraums, Cambridge Univ. Press, Cambridge, 45–74.

Taylor, K., 1976. The influence of subsurface energy storage on seasonal temperature variations. *J. Appl. Meteorol.,* **15**, 1129–1138.

Tricot, Ch., 1989. The transient response of climate to greenhouse gas concentration changes: a preliminary study with a two-dimensional coupled atmosphere–ocean model. *Our Changing Atmosphere, Proceedings of the 28th Liège International Colloquium.* Edited by P. J. Crutzen, J. C. Gérard, and R. Zander, Université de Liège, Liège, 333–338.

Tricot, Ch., and A. Berger, 1988. Sensitivity of present-day climate to astronomical forcing. *Long and Short Term Variability of Climate, Lecture Notes in Earth Sciences,* vol.16. Edited by H. Wanner and U. Siegenthaler, 132–152.

White, A. A., and J. S. A. Green, 1984. Transfer coefficient eddy flux parameterizations in a simple model of the zonal average atmospheric circulation. *Quart. J. R. Met. Soc.*, **110**, 1035–1052.

Wigley, T. M. L., and S. C. B. Raper, 1990. Climatic change due to solar irradiance changes. *Geophys. Res. Lett.*, **17**, 2169–2172.

Willson, R. C., S. Gulkis, M. Janssen, M. S. Hudson, and G. A. Chapman, 1981. Observations of solar irradiance variability. *Science*, **211**, 700–702.

Willson, R. C., and H. S. Hudson, 1988. Solar luminosity variations in solar cycle 21. *Nature*, **332**, 810–812.

Wilson, C. A., and J. F. B. Mitchell, 1987. A doubled $CO_2$ climate sensitivity experiment with a global climate model including a simple ocean. *J. Geophys. Res.*, **92**, 13,315–13,343.